53rd IEEE Conference on Decision and Control
December 15-17, 2014. Los Angeles, California, USA

Exploration and Mapping of an Unknown Flight Envelope

Ahmad Ansari, Ming-Jui Yu, and Dennis S. Bernstein

Abstract— **The flight envelope of an aircraft consists of the constant trim states that the aircraft can attain, given in terms of airspeed, turn rate, and flight path angle. Flight trajectories typically consist of a sequence of trim commands with intermediate transitions. While the flight envelope of an aircraft is determined beforehand, it may change under off-nominal conditions due to damage or actuator failure. The goal of this paper is to investigate the ability of an adaptive control law to reach new trim states in the case where the flight envelope is totally unknown. Within simulation, this approach provides an alternative technique for mapping the flight envelope. For an aircraft in flight, this approach can be used to reach new trim states under envelope uncertainty, as may occur during off-nominal flight conditions.**

I. Introduction

Emergency flight control depends on the ability of the pilot and autopilot to maintain effective control of the aircraft despite highly uncertain and constrained circumstances. Damage to the aircraft structure, as well as malfunctioning engines, control surfaces, and sensors, are potential hazards to safe handling of the aircraft [1, 2].

The flight envelope of an aircraft is the set of trim values that it can attain and maintain during flight. These include airspeed, turn rate, and flight path angle. All aircraft have a fully characterized flight envelope for safe flight, and the flight trajectory of an aircraft typically consists of a sequence of trim commands with intermediate transitions.

The flight envelope of an aircraft can be determined by solving the nonlinear algebraic equations for the trim equilibria [3]. These equations depend on detailed knowledge of the aircraft aerodynamics. In an emergency flight situation, however, the aerodynamics may be different from those of the nominal aircraft, in which case the flight envelope is unknown.

One approach to dealing with an unknown flight envelope is to apply adaptive control methods. This approach is used in [4], where the flight envelope is assumed to be unknown outside of a well-characterized region. Along the same lines, retrospective cost adaptive control (RCAC) [5–7] is used in [8] to follow trim commands without knowledge of whether or not the trim commands fall within the flight envelope. As shown in [8], RCAC may reach a trim state that is different from the commanded trim if, for example, the commanded angle of attack or commanded airspeed are outside the envelope of the aircraft.

The goal of the present paper is to go beyond [8] by systematically investigating the ability of RCAC to reach a commanded trim with no knowledge about the flight envelope of the aircraft. To do this, we consider an aircraft flying in a trim condition, at which time an alternative trim command is issued without knowledge of whether or not the commanded trim is within the aircraft flight envelope. The only modeling information used by RCAC is a single Markov parameter of the dynamics at the present trim condition. Using the NASA GTM model [9, 10] we simulate the closed-loop response using RCAC. All simulations are fully nonlinear based on an aerodynamic lookup table.

The trims that are reachable under these conditions can be viewed in two ways. First, within a simulation environment, and without flying an actual aircraft, the reachable trims provide an estimate of the flight envelope. This mapping technique may be useful either as an alternative to solving the algebraic equations or as a way of validating the results of the numerical solution. Secondly, the reachable trims can provide an indication of what is achievable by the real aircraft under conditions of an unknown flight envelope, as may occur in an emergency situation.

The contents of the paper are as follows. We first review RCAC and provide definitions for trim flight. We then describe the methodology for mapping the flight envelope, providing examples of stable and unstable trims. Finally, we describe the achieved flight envelope and provide a means of expanding the search method.

II. Adaptive Controller Design

A. Problem Formulation

Consider the MIMO discrete-time system

$$x(k+1) = Ax(k) + Bu(k) + D_1 w(k), \tag{1}$$
$$y(k) = Cx(k) + D_2 w(k), \tag{2}$$
$$z(k) = E_1 x(k) + E_0 w(k), \tag{3}$$

where $x(k) \in \mathbb{R}^n$, $y(k) \in \mathbb{R}^{l_y}$, $z(k) \in \mathbb{R}^{l_z}$, $u(k) \in \mathbb{R}^{l_u}$, $w(k) \in \mathbb{R}^{l_w}$, and $k \geq 0$. Our goal is to develop an adaptive output feedback controller that minimizes the performance variable z in the presence of the exogenous signal w with minimal modeling information about the dynamics and w. Note that w can represent either a command signal to be followed, an external disturbance to be rejected, or both. The system (1)–(3) can represent a sampled-data application arising from a continuous-time system with sample and hold operations.

If $D_1 = 0$ and $E_0 \neq 0$, then the objective is to have the output $E_1 x$ follow the command signal $-E_0 w$. On the other hand, if $D_1 \neq 0$ and $E_0 = 0$, then the objective is to reject the disturbance w from the performance measurement

Ahmad Ansari, Ming-Jui Yu, and D. S. Bernstein are with the Department of Aerospace Engineering, University of Michigan, Ann Arbor, MI, USA. {ansahmad, mingray, dsbaero}@umich.edu

E_1x. Furthermore, if $D_1 = \left[\begin{array}{cc}\hat{D}_1 & 0\end{array}\right]$, $E_0 = \left[\begin{array}{cc}0 & \hat{E}_0\end{array}\right]$, and $w(k) = \left[\begin{array}{cc}w_1(k)^{\mathrm{T}} & w_2(k)^{\mathrm{T}}\end{array}\right]^{\mathrm{T}}$, then the objective is to have E_1x follow the command $-\hat{E}_0w_2$ while rejecting the disturbance w_1. Lastly, if D_1 and E_0 are empty matrices, then the objective is output stabilization, that is, convergence of z to zero.

B. Retrospective Cost

For $i \geq 1$, define the Markov parameter of G_{zu} given by

$$H_i \triangleq E_1A^{i-1}B. \tag{4}$$

For example, $H_1 = E_1B$ and $H_2 = E_1AB$. Let r be a positive integer. Then, for all $k \geq r$,

$$x(k) = A^r x(k-r) + \sum_{i=1}^{r} A^{i-1}Bu(k-i) + \sum_{i=1}^{r} A^{i-1}D_1w(k-i), \tag{5}$$

and thus

$$z(k) = E_1A^r x(k-r) + \sum_{i=1}^{r} E_1A^{i-1}D_1w(k-i) + E_0w(k) + \bar{H}\bar{U}(k-1), \tag{6}$$

where

$$\bar{H} \triangleq \left[\begin{array}{ccc} H_1 & \cdots & H_r \end{array}\right] \in \mathbb{R}^{l_z \times rl_u}$$

and

$$\bar{U}(k-1) \triangleq \left[\begin{array}{c} u(k-1) \\ \vdots \\ u(k-r) \end{array}\right].$$

Next, we rearrange the columns of $\bar{H}$ and the components of $\bar{U}(k-1)$ and partition the resulting matrix and vector so that

$$\bar{H}\bar{U}(k-1) = \mathcal{H}'U'(k-1) + \mathcal{H}U(k-1), \tag{7}$$

where $\mathcal{H}' \in \mathbb{R}^{l_z \times (rl_u - l_U)}$, $\mathcal{H} \in \mathbb{R}^{l_z \times l_U}$, $U'(k-1) \in \mathbb{R}^{rl_u - l_U}$, and $U(k-1) \in \mathbb{R}^{l_U}$. Then, we can rewrite (6) as

$$z(k) = \mathcal{S}(k) + \mathcal{H}U(k-1), \tag{8}$$

where

$$\mathcal{S}(k) \triangleq E_1A^r x(k-r) + \sum_{i=1}^{r} E_1A^{i-1}D_1w(k-i) + E_0w(k) + \mathcal{H}'U'(k-1). \tag{9}$$

Next, for $j = 1, \ldots, s$, we rewrite (8) with a delay of k_j time steps, where $0 \leq k_1 \leq k_2 \leq \cdots \leq k_s$, in the form

$$z(k-k_j) = \mathcal{S}_j(k-k_j) + \mathcal{H}_jU_j(k-k_j-1), \tag{10}$$

where (9) becomes

$$\mathcal{S}_j(k-k_j) \triangleq E_1A^r x(k-k_j-r) + \sum_{i=1}^{r} E_1A^{i-1}D_1w(k-k_j-i) + E_0w(k-k_j) + \mathcal{H}'_jU'_j(k-k_j-1)$$

and (7) becomes

$$\bar{H}\bar{U}(k-k_j-1) = \mathcal{H}'_jU'_j(k-k_j-1) + \mathcal{H}_jU_j(k-k_j-1), \tag{11}$$

where $\mathcal{H}'_j \in \mathbb{R}^{l_z \times (rl_u - l_{U_j})}$, $\mathcal{H}_j \in \mathbb{R}^{l_z \times l_{U_j}}$, $U'_j(k-k_j-1) \in \mathbb{R}^{rl_u - l_{U_j}}$, and $U_j(k-k_j-1) \in \mathbb{R}^{l_{U_j}}$. Now, by stacking $z(k-k_1), \ldots, z(k-k_s)$, we define the *extended performance*

$$Z(k) \triangleq \left[\begin{array}{c} z(k-k_1) \\ \vdots \\ z(k-k_s) \end{array}\right] \in \mathbb{R}^{sl_z}. \tag{12}$$

Therefore,

$$Z(k) = \tilde{\mathcal{S}}(k) + \tilde{\mathcal{H}}\tilde{U}(k-1), \tag{13}$$

where

$$\tilde{\mathcal{S}}(k) \triangleq \left[\begin{array}{c} \mathcal{S}_1(k-k_1) \\ \vdots \\ \mathcal{S}_s(k-k_s) \end{array}\right] \in \mathbb{R}^{sl_z}, \tag{14}$$

$\tilde{U}(k-1)$ has the form

$$\tilde{U}(k-1) \triangleq \left[\begin{array}{c} u(k-q_1) \\ \vdots \\ u(k-q_{l_{\tilde{U}}}) \end{array}\right] \in \mathbb{R}^{l_{\tilde{U}}}, \tag{15}$$

where, for $i = 1, \ldots, l_{\tilde{U}}$, $k_1 \leq q_i \leq k_s + r$, and $\tilde{\mathcal{H}} \in \mathbb{R}^{sl_z \times l_{\tilde{U}}}$ is constructed according to the structure of $\tilde{U}(k-1)$. The vector $\tilde{U}(k-1)$ is formed by stacking $U_1(k-k_1-1), \ldots, U_s(k-k_s-1)$ and removing copies of repeated components.

Next, we define the *retrospective performance*

$$\hat{z}(k-k_j) \triangleq \mathcal{S}_j(k-k_j) + \mathcal{H}_j\hat{U}_j(k-k_j-1), \tag{16}$$

where the past controls $U_j(k-k_j-1)$ in (10) are replaced by the retrospective controls $\hat{U}_j(k-k_j-1)$. In analogy with (12), we define

$$\hat{Z}(k) \triangleq \left[\begin{array}{c} \hat{z}(k-k_1) \\ \vdots \\ \hat{z}(k-k_s) \end{array}\right] \in \mathbb{R}^{sl_z} \tag{17}$$

and thus

$$\hat{Z}(k) = \tilde{\mathcal{S}}(k) + \tilde{\mathcal{H}}\hat{\tilde{U}}(k-1), \tag{18}$$

where the components of $\hat{\tilde{U}}(k-1) \in \mathbb{R}^{l_{\tilde{U}}}$ are the components of $\hat{U}_1(k-k_1-1), \ldots, \hat{U}_s(k-k_s-1)$ ordered in the same way as the components of $\tilde{U}(k-1)$. Subtracting (13) from (18) yields

$$\hat{Z}(k) = Z(k) - \tilde{\mathcal{H}}\tilde{U}(k-1) + \tilde{\mathcal{H}}\hat{\tilde{U}}(k-1). \tag{19}$$

Finally, we define the *retrospective cost function*

$$J(\hat{\hat{U}}(k-1),k) \triangleq \hat{Z}^{\mathrm{T}}(k)R(k)\hat{Z}(k), \tag{20}$$

where $R(k) \in \mathbb{R}^{l_z s \times l_z s}$ is a positive-definite performance weighting. The goal is to determine refined controls $\hat{\hat{U}}(k-1)$ that would have provided better performance than the controls $U(k)$ that were applied to the system. The refined control values $\hat{\hat{U}}(k-1)$ are subsequently used to update the controller.

C. Cost Function Optimization with Adaptive Regularization

To ensure that (20) has a global minimizer, we consider the regularized cost

$$\begin{aligned}\bar{J}(\hat{\hat{U}}(k-1),k) \triangleq\ & \hat{Z}^{\mathrm{T}}(k)R(k)\hat{Z}(k)\\ &+ \eta(k)R_2\hat{\hat{U}}^{\mathrm{T}}(k-1)\hat{\hat{U}}(k-1),\end{aligned} \tag{21}$$

where $\eta(k) \geq 0$, and $R_2 \in \mathbb{R}^{\hat{\hat{U}}} \geq 0$. Substituting (19) into (21) yields

$$\begin{aligned}\bar{J}(\hat{\hat{U}}(k-1),k) =\ & \hat{\hat{U}}(k-1)^{\mathrm{T}}\mathcal{A}(k)\hat{\hat{U}}(k-1)\\ &+ \hat{\hat{U}}^{\mathrm{T}}(k-1)\mathcal{B}^{\mathrm{T}}(k) + \mathcal{C}(k),\end{aligned} \tag{22}$$

where

$$\mathcal{A}(k) \triangleq \tilde{\mathcal{H}}^{\mathrm{T}}R(k)\tilde{\mathcal{H}} + \eta(k)R_2 I_{l_{\tilde{U}}}, \tag{23}$$

$$\mathcal{B}(k) \triangleq 2\tilde{\mathcal{H}}^{\mathrm{T}}R(k)[Z(k) - \tilde{\mathcal{H}}\tilde{U}(k-1)], \tag{24}$$

$$\begin{aligned}\mathcal{C}(k) \triangleq\ & Z^{\mathrm{T}}(k)R(k)Z(k) - 2Z^{\mathrm{T}}(k)R(k)\tilde{\mathcal{H}}\tilde{U}(k-1)\\ &+ \tilde{U}^{\mathrm{T}}(k-1)\tilde{\mathcal{H}}^{\mathrm{T}}R(k)\tilde{\mathcal{H}}\tilde{U}(k-1).\end{aligned} \tag{25}$$

If either $\tilde{\mathcal{H}}$ has full column rank or $\eta(k) > 0$ and $R_2 > 0$, then $\mathcal{A}(k)$ is positive definite. In this case, $\bar{J}(\hat{\hat{U}}(k-1),k)$ has the unique global minimizer

$$\hat{\hat{U}}(k-1) = -\frac{1}{2}\mathcal{A}^{-1}(k)\mathcal{B}(k). \tag{26}$$

D. Controller Construction

The control $u(k)$ is given by the strictly proper time-series controller of order n_{c} given by

$$u(k) = \sum_{i=1}^{n_{\mathrm{c}}} M_i(k)u(k-i) + \sum_{i=1}^{n_{\mathrm{c}}} N_i(k)y(k-i), \tag{27}$$

where, for all $i = 1,\dots,n_{\mathrm{c}}$, $M_i(k) \in \mathbb{R}^{l_u \times l_u}$ and $N_i(k) \in \mathbb{R}^{l_u \times l_y}$. The control (27) can be expressed as

$$u(k) = \theta(k)\phi(k-1), \tag{28}$$

where

$$\begin{aligned}\theta(k) \triangleq [&M_1(k)\ \cdots\ M_{n_{\mathrm{c}}}(k)\\ &N_1(k)\ \cdots\ N_{n_{\mathrm{c}}}(k)] \in \mathbb{R}^{l_u \times n_{\mathrm{c}}(l_u+l_z)}\end{aligned} \tag{29}$$

and

$$\phi(k-1) \triangleq \begin{bmatrix} u(k-1)\\ \vdots\\ u(k-n_{\mathrm{c}})\\ y(k-1)\\ \vdots\\ y(k-n_{\mathrm{c}}) \end{bmatrix} \in \mathbb{R}^{n_{\mathrm{c}}(l_u+l_y)}. \tag{30}$$

E. Recursive Least Squares Update of $\theta(k)$

Next, let d be a positive integer such that $\tilde{U}(k-1)$ contains $u(k-d)$ and define the cumulative cost function

$$\begin{aligned}J_{\mathrm{R}}(\theta,k) \triangleq & \sum_{i=d+1}^{k} \lambda^{k-i}\|\phi^{\mathrm{T}}(i-d-1)\theta^{\mathrm{T}}(k) - \hat{u}^{\mathrm{T}}(i-d)\|^2\\ &+ \lambda^k(\theta(k)-\theta_0)P_0^{-1}(\theta(k)-\theta_0)^{\mathrm{T}},\end{aligned} \tag{31}$$

where $\|\cdot\|$ is the Euclidean norm, and $\lambda \in (0,1]$ is the forgetting factor. Minimizing (31) yields

$$\begin{aligned}\theta^{\mathrm{T}}(k) =\ & \theta^{\mathrm{T}}(k-1) + \beta(k)P(k-1)\phi(k-d-1)\\ &\cdot[\phi^{\mathrm{T}}(k-d)P(k-1)\phi(k-d-1) + \lambda(k)]^{-1}\\ &\cdot[\phi^{\mathrm{T}}(k-d-1)\theta^{\mathrm{T}}(k-1) - \hat{u}^{\mathrm{T}}(k-d)],\end{aligned}$$

where $\beta(k)$ is either zero or one. The error covariance is updated by

$$\begin{aligned}P(k) =\ & \beta(k)\lambda^{-1}P(k-1) + [1-\beta(k)]P(k-1)\\ &- \beta(k)\lambda^{-1}P(k-1)\phi(k-d-1)\\ &\cdot[\phi^{\mathrm{T}}(k-d-1)P(k-1)\phi(k-d) + \lambda]^{-1}\\ &\cdot\phi^{\mathrm{T}}(k-d-1)P(k-1).\end{aligned}$$

We initialize the error covariance matrix as $P(0) = \alpha I_{3n_{\mathrm{c}}}$, where $\alpha > 0$. Note that when $\beta(k) = 0$, $\theta(k) = \theta(k-1)$ and $P(k) = P(k-1)$. Therefore, setting $\beta(k) = 0$ switches off the controller adaptation, and thus freezes the control gains. When $\beta(k) = 1$, the controller is allowed to adapt.

III. Definition of Trim Flight

Denote the Earth inertial frame and the aircraft body-fixed frame by $\mathrm{F_E}$ and $\mathrm{F_{AC}}$, respectively. The translational and angular velocity of an aircraft resolved in the aircraft body-fixed frame are given by

$$\begin{bmatrix} U\\ V\\ W \end{bmatrix} \triangleq \vec{V}_{\mathrm{AC}}\Big|_{\mathrm{AC}}, \quad \begin{bmatrix} P\\ Q\\ R \end{bmatrix} \triangleq \vec{\omega}_{\mathrm{AC/E}}\Big|_{\mathrm{AC}}. \tag{32}$$

We define *steady flight* as aircraft flight with constant U,V,W,P,Q,R. *Airspeed* V_{AC} is defined as the magnitude of the velocity vector, that is,

$$V_{\mathrm{AC}} = |\vec{V}_{\mathrm{AC}}| = \sqrt{U^2+V^2+W^2}. \tag{33}$$

Flight path angle γ is defined as the angle between $\vec{V}_{\mathrm{AC}}$ and its projection onto the horizontal $\hat{\imath}_{\mathrm{E}}$-$\hat{\jmath}_{\mathrm{E}}$ plane.

We define the *orientation matrix* of $\mathrm{F_{AC}}$ relative to $\mathrm{F_E}$ by

$$\mathcal{O}_{\mathrm{AC/E}} \triangleq \vec{R}_{\mathrm{AC/E}}\Big|_{\mathrm{AC}}^{\mathrm{T}}. \tag{34}$$

We then resolve the angular velocity in $\mathrm{F_E}$ by noting that

$$\begin{aligned}\vec{\omega}_{\mathrm{AC/E}}\Big|_{\mathrm{E}} &= \mathcal{O}_{\mathrm{AC/E}}^{\mathrm{T}}\, \vec{\omega}_{\mathrm{AC/E}}\Big|_{\mathrm{AC}} = \mathcal{O}_{\mathrm{E/AC}}\, \vec{\omega}_{\mathrm{AC/E}}\Big|_{\mathrm{AC}} \\ &= \mathcal{O}_{\mathrm{E/E'}}\mathcal{O}_{\mathrm{E'/E''}}\mathcal{O}_{\mathrm{E''/AC}}\, \vec{\omega}_{\mathrm{AC/E}}\Big|_{\mathrm{AC}},\end{aligned} \tag{35}$$

and we define

$$\begin{bmatrix} P_{\mathrm{E}} \\ Q_{\mathrm{E}} \\ R_{\mathrm{E}} \end{bmatrix} \triangleq \vec{\omega}_{\mathrm{AC/E}}\Big|_{\mathrm{E}}. \tag{36}$$

Turn rate is R_{E}. Note that P, Q, R are constant if and only if P_{E}, Q_{E}, R_{E} are constant. *Trim flight* is defined as steady flight with constant flight path angle. Constant-airspeed flight in a vertical circle is steady, but not a trim. During trim flight, forces on the aircraft are constant and balanced, and control surface deflection and throttle settings are constant. There are 6 possible types of trim flights: level straight-line flight, ascending straight-line flight, descending straight-line flight, level turning flight, rising helical flight, and descending helical flight.

IV. Flight Envelope Exploration and Mapping

We use RCAC to explore and map the flight envelope of the NASA Generic Transport Model (GTM). GTM is a fully nonlinear aircraft model with 6 degrees of freedom and 12 states [9, 10].

In all examples, the aircraft is commanded to follow constant airspeed, flight path angle, and turn rate. In addition, U, V, W, P, Q, R are constant in all cases, resulting in trim commands.

The flight envelope exploration scheme iterates through the following sequence of commands to maneuver the aircraft around the flight envelope and determine the stability of the attained trim states:

1) Start the aircraft at an initial trim condition.
2) Choose a trim command.
3) Increase or decrease the airspeed to the desired value by a sequence of intermediate ramp commands with slope of 0.1 $\mathrm{ft/sec^2}$ and sufficient dwell time for the aircraft to reach the command.
4) Increase or decrease the turn rate to the desired value by a sequence of intermediate ramp commands with slope of 0.1 $\mathrm{deg/sec^2}$ and sufficient dwell time for the aircraft to reach the command.
5) After reaching the desired trim, return to open-loop flight by shutting off the controller and freezing all actuators and throttle settings.
6) Impulse the elevator and rudder to observe the stability of the aircraft at the new trim state..

For all commands, one tuning is used for the adaptive controller, namely,

$$\begin{aligned}&\tilde{\mathcal{H}} = [H_1\ H_2], n_c = 16, P_0 = 0.03, \\ &\eta_0 = [\ 0.0001 \quad 0.0001 \quad 0.005 \quad 0.01 \quad 0.01\ ].\end{aligned} \tag{37}$$

The values of η_0 used for the 5 actuators correspond to left throttle, right throttle, elevator, aileron, and rudder, respectively. We initialize the controller parameter θ to stabilize the aircraft at the initial trim condition.

A. Stability of Trim

Since each trim flight is an equilibrium produced by constant forcing, it is natural to investigate its open-loop stability. Figure 1 shows the adaptive controller maneuvering the aircraft to an asymptotically stable trim. The aircraft has an initial airspeed of 67.3 ft/sec, turn rate of 0 deg/sec, and flight path angle of 0 deg. Ramp commands are first given in airspeed and then in turn rate until the aircraft reaches the airspeed of 82.3 ft/sec and turn rate of 10 deg/sec. Flight path angle is commanded to remain at 0 deg throughout. At t = 9800 sec, the controller is shut off and all actuators and throttle settings are kept constant. An impulse in the elevator and rudder is given at t = 10300 sec, and the aircraft immediately returns to the commanded trim state. Figure 2 displays the trajectory of the aircraft.

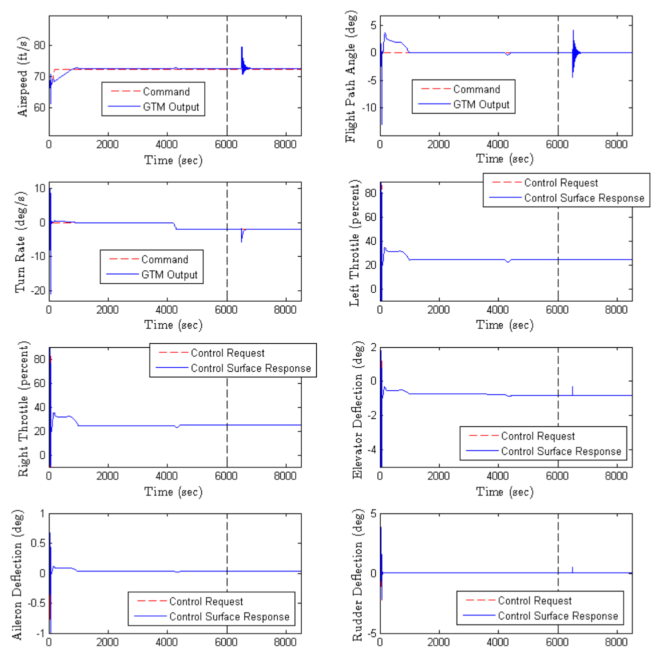

Fig. 1. RCAC maneuvers the aircraft to an asymptotically stable trim using a sequence of ramp commands with sufficient dwell time for convergence. At t = 9800 sec, denoted by the vertical dashed black line, the controller is shut off and all actuators are kept constant. After being impulsed at t = 10300 sec, the aircraft returns to the new trim state.

Figure 3 shows the adaptive controller maneuvering the aircraft to an asymptotically stable trim. The aircraft has an initial airspeed of 67.3 ft/sec, turn rate of 0 deg/sec, and flight path angle of 0 deg. Ramp commands are first given in airspeed and then in turn rate until the aircraft reaches an airspeed of 62.3 ft/sec and turn rate of 6 deg/sec. Flight path angle is commanded to remain at 0 deg throughout.

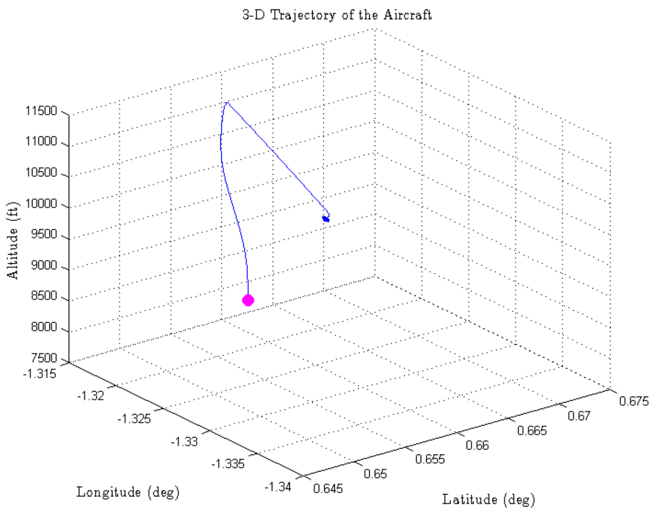

Fig. 2. Trajectory of the aircraft as it maneuvers towards the aymptotically stable trim state. The initial trim is denoted by a magenta dot.

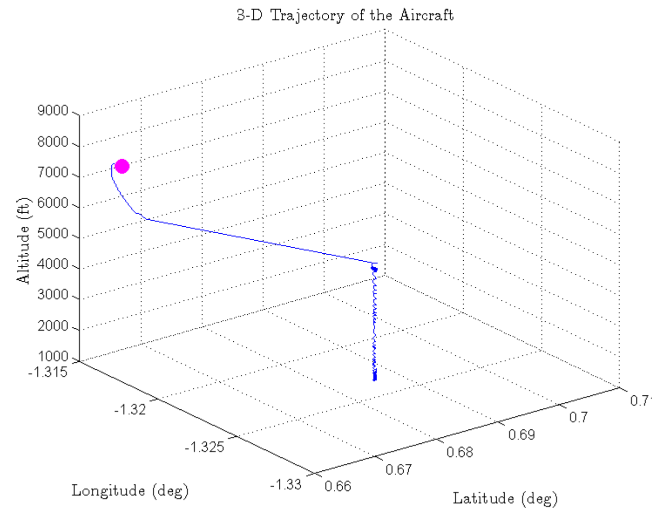

Fig. 4. Trajectory of the aircraft as it maneuvers towards the trim state that is not asymptotically stable. The initial trim is denoted by a magenta dot.

At t = 9800 sec, the controller is shut off and all actuators and throttle settings are kept constant. An impulse in the elevator and rudder is given at t = 10300 sec, and the aircraft immediately begins to oscillate about the commanded trim state. Figure 4 displays the trajectory of the aircraft.

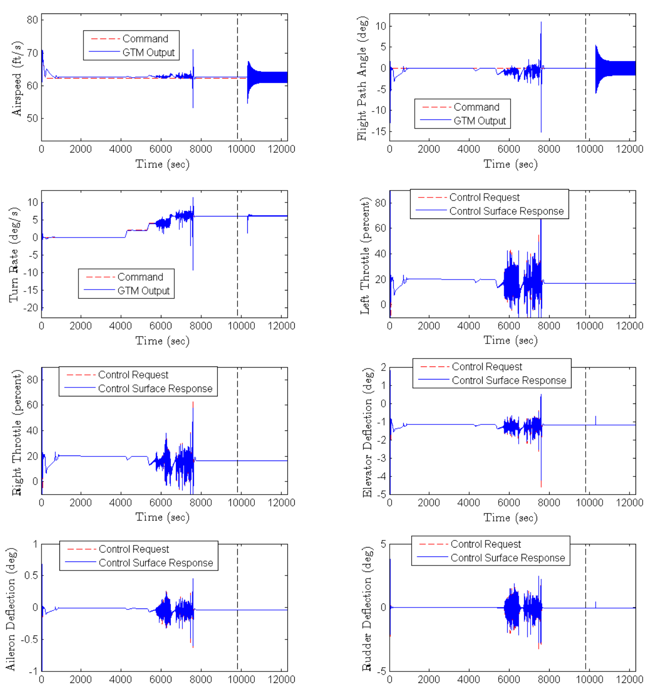

Fig. 3. RCAC maneuvers the aircraft to a trim that is not asymptotically stable using a sequence of ramp commands with sufficient dwell time for convergence. At t = 9800 sec, denoted by the vertical dashed black line, the controller is shut off and all actuators are kept constant. After being impulsed at t = 10300 sec, the aircraft begins to oscillate about the commanded trim.

B. Attained Flight Envelope and Further Exploration

Figure 5 shows the mapping of the flight envelope after the exploration scheme is completed. Starting from the initial condition of $V = 67.3$ ft/sec, $R_{\rm E} = 0$ deg/sec, and $\gamma =$ 0 deg, we search through a slice of the flight envelope by keeping flight path angle constant while varying airspeed and turn rate, as indicated by the magenta arrows. The region of attained trim states consists mainly of asymptotically stable trims, with trims that are not asymptotically stable at the boundary. The trims that are not asymptotically stable are actively stabilized by the adaptive controller.

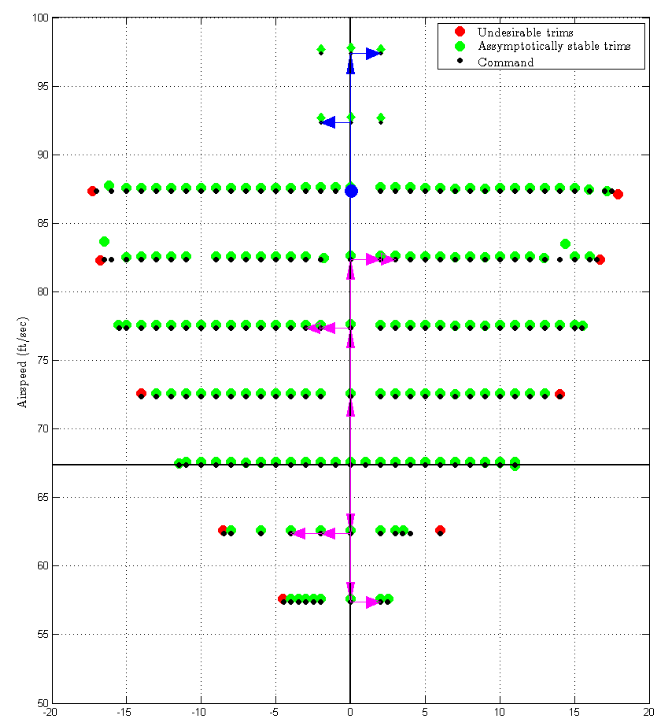

Fig. 5. Region of attained trim states starting from the same initial condition and keeping turn rate constant. Further exploration starting from another initial condition, indicated by the blue dot, is also shown.

There are three possible outcomes when the aircraft is commanded outside the region of attained trims. When commanded to reach an airspeed above the region, the aircraft converges to a different trim within the flight envelope. This behavior is shown in Figure 6. When commanded to reach an airspeed below the region, the aircraft may exhibit the same behavior shown in Figure 6 or it may exhibit an oscillatory behavior around the command, as shown in Figure 7. When commanded to reach a turn rate outside the attained flight envelope, the aircraft may exhibit the behavior shown in Figure 7 or it may be unstable.

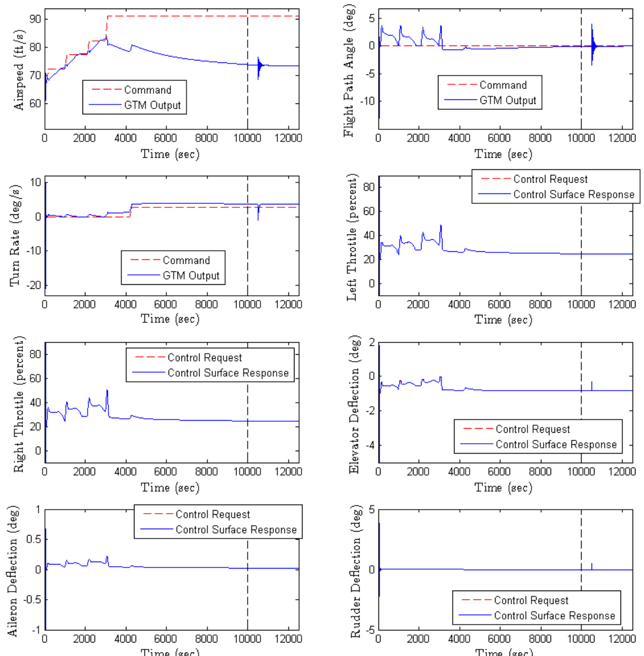

Fig. 6. RCAC maneuvers the aircraft to a trim with airspeed above the region of attained trims. The aircraft does not reach the command, instead traversing to a trim within the region.

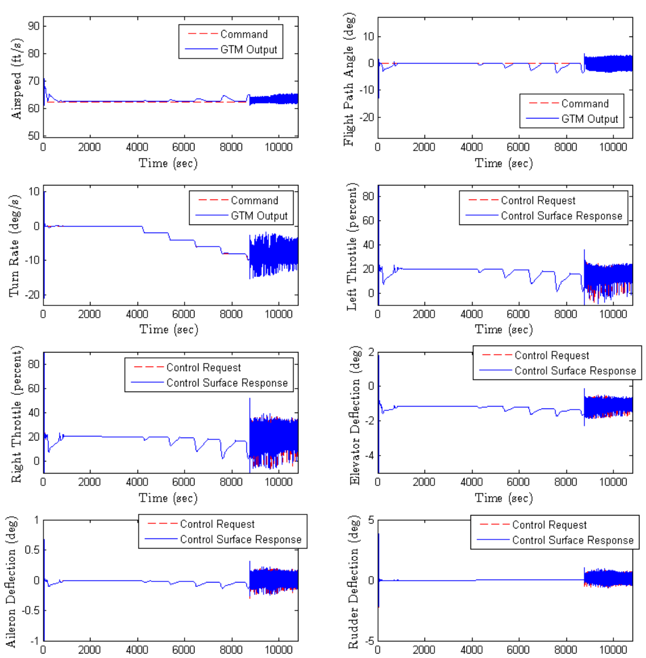

Fig. 7. RCAC maneuvers the aircraft to a trim with airspeed below the region of attained trims. The aircraft reaches the command but begins to oscillate about it.

All attained trims in Figure 5 are reached from the same initial condition and initial controller parameters. To increase the possible regions of exploration, we begin a new flight envelope exploration and mapping procedure from an initial airspeed of 87.3 ft/sec, turn rate of 0 deg/sec, and flight path angle of 0 deg. This initial condition is at the boundary of the previous mapping, as indicated by the blue dot in Figure 5, and from there we traverse outside the region of attained trims corresponding to the first initial condition.

V. Conclusions

In this paper, we applied RCAC to the GTM for the purpose of exploring an unknown flight envelope. Using knowledge of the first 2 Markov parameters of the linearized model about the initial trim condition, we were able to systematically maneuver the aircraft through a range of trim states, including both trims that are asymptotically stable and trims that require active stabilization. By changing the initial trim condition and initial controller parameters, we also demonstrated the ability to further expand the region of attainable trim states.

VI. Future Work

The next step in this research is to explore and map different slices of the flight envelope in order to map out the full 3-dimensional flight envelope. We will then compare the obtained flight envelope with the true flight envelope of the aircraft.

References

[1] L. Tang, M. Roemer, J. Ge, A. Crassidis, J. V. R. Prasad, and C. Belcastro, "Methodologies for adaptive flight envelope estimation and protection," in *Proc. AIAA Guid. Nav. Contr. Conf.*, Chicago, IL, August 2009, AIAA-2009-6260.

[2] R. C. Allen and H. G. Kwatny, "Maneuverability and envelope protection in the prevention of aircraft loss of control," in *Proc. IEEE Asian Contr. Conf.*, Kaohsiung, Taiwan, May 2011, pp. 381–386.

[3] N. H. McClamroch, *Steady Aircraft Flight and Performance*. Princeton University Press, 2011.

[4] N. Hovakimyan, C. Cao, E. Kharisov, E. Xargay, and I. Gregory, "L1 adaptive controller for safety critical systems: Guaranteed robustness with fast adaptation," *IEEE Contr. Sys. Mag.*, pp. 54–104, October 2011.

[5] R. Venugopal and D. S. Bernstein, "Adaptive Disturbance Rejection Using ARMARKOV System Representations," *IEEE Trans. Contr. Sys. Tech.*, vol. 8, pp. 257–269, 2000.

[6] J. B. Hoagg, M. A. Santillo, and D. S. Bernstein, "Discrete-time adaptive command following and disturbance rejection for minimum phase systems with unknown exogenous dynamics," *IEEE Trans. Autom. Contr.*, vol. 53, pp. 912–928, 2008.

[7] J. Hoagg and D. Bernstein, "Retrospective cost model reference adaptive control for nonminimum-phase systems," *AIAA J. Guid. Contr. Dyn.*, vol. 35, pp. 1767–1786, 2012.

[8] M. J. Yu, J. Zhong, E. M. Atkins, I. V. Kolmanovsky, and D. S. Bernstein, "Trim-commanded adaptive control for waypoint-defined trajectory following," in *Proc. AIAA Guid. Nav. Contr. Conf.*, Boston, MA, August 2013, AIAA-2013-5000.

[9] D. Cox, "The GTM DesignSim r415," 2008.

[10] R. M. Bailey, R. W. Hostetler, K. N. Barnes, C. M. Belcastro, and C. M. Belcastro, "Experimental validation: Subscale aircraft ground facilities and integrated test capability," in *Proc. AIAA Guid. Nav. Cont. Conf.*, San Francisco, CA, August 2005, AIAA-2005-6433.